

Charmonium dissociation in collision with ϕ meson in hadronic matter

Shi-Tao Ji* and Xiao-Ming Xu

Department of Physics, Shanghai University, Baoshan, Shanghai 200444, China

Abstract

The ϕ -charmonium dissociation reactions in hadronic matter are studied. Unpolarised cross sections for $\phi J/\psi \rightarrow D_s^- D_s^+$, $\phi J/\psi \rightarrow D_s^{*-} D_s^+$ or $D_s^- D_s^{*+}$, $\phi J/\psi \rightarrow D_s^{*-} D_s^{*+}$, $\phi \psi' \rightarrow D_s^- D_s^+$, $\phi \psi' \rightarrow D_s^{*-} D_s^+$ or $D_s^- D_s^{*+}$, $\phi \psi' \rightarrow D_s^{*-} D_s^{*+}$, $\phi \chi_c \rightarrow D_s^- D_s^+$, $\phi \chi_c \rightarrow D_s^{*-} D_s^+$ or $D_s^- D_s^{*+}$ and $\phi \chi_c \rightarrow D_s^{*-} D_s^{*+}$ are calculated in the Born approximation, in the quark-interchange mechanism and with a temperature-dependent quark potential. The potential leads to remarkable temperature dependence of the cross sections. With the cross sections and the ϕ distribution function we calculate the dissociation rates of the charmonia in the interactions with the ϕ meson in hadronic matter. The dependence of the rates on temperature and charmonium momentum is meaningful to the influence of ϕ mesons on charmonium suppression.

PACS numbers: 25.75.-q, 24.85.+p, 12.38.Mh

Keywords: Charmonium dissociation cross sections, Quark-interchange mechanism, Dissociation rate

*Electronic address: 459756153@qq.com; Fax: +86 21 66134208

I. INTRODUCTION

Hadronic matter affects production of particles in relativistic heavy-ion collisions. Change of J/ψ in hadronic matter is appreciable. The change of J/ψ number is caused by inelastic meson-charmonium scattering [1–5] and spontaneous dissociation that may happen when temperature is higher than the J/ψ dissociation temperature [6]. Studies of charmonium dissociation in collisions with hadrons are important in the field of relativistic heavy-ion collisions. Since the ϕ -meson production is enhanced in Au-Au collisions at Relativistic Heavy Ion Collider energies, it is interesting to investigate ϕ -charmonium dissociation in hadronic matter. This is the subject of this paper.

We calculate ϕ -charmonium dissociation cross sections in the Born approximation and in the quark-interchange mechanism [7]. The quark interchange mechanism between the incident meson and the charmonium breaks the charmonium and produces charmed mesons and/or charmed strange mesons. Dissociation of charmonia in collisions with π , ρ and K in vacuum has been studied in Ref. [3] and dissociation in hadronic matter in Refs. [4, 5]. Meson-charmonium dissociation cross sections in hadronic matter differ from those in vacuum. The in-vacuum cross sections obtained in the quark-interchange approach are different from the cross sections obtained in the meson-exchange approach [1] and in the short-distance approach [2]. The ϕ -charmonium dissociation cross sections have not been calculated in the quark-interchange approach, in the meson-exchange approach and in the short-distance approach.

With the ϕ -charmonium dissociation cross sections we calculate the dissociation rate of the charmonium in the interaction with the ϕ meson in hadronic matter. The larger the dissociation rate is, the stronger charmonium suppression ϕ mesons cause. From the dissociation rate we can understand contribution of the ϕ meson to the charmonium suppression. Therefore, the second task of the paper is to calculate the dissociation rate.

The remainder of this paper is organized as follows. In Section II formulas for the dissociation cross section and the dissociation rate are presented. In Section III we show numerical results of unpolarised ϕ -charmonium dissociation cross sections and charmonium dissociation rates. Relevant discussions are given. A summary is in Section IV.

II. CROSS-SECTION AND DISSOCIATION-RATE FORMULAS

The scattering $A(s\bar{s}) + B(c\bar{c}) \rightarrow C(s\bar{c}) + D(c\bar{s})$ takes place due to quark interchange and interactions among constituents (quarks and antiquarks). The scattering has the two forms, the prior form and the post form. The scattering in the prior form means that gluon exchange occurs before quark interchange. The scattering in the post form contains gluon exchange after quark interchange. The scattering in the two forms is depicted in Figs. 1 and 2 in Ref. [5]. Cross-section formulas for the scattering are given in Refs. [4, 8]. Here we briefly introduce the formulas. Application of the cross section to get the charmonium dissociation rate follows.

Denote the spin, orbital angular momentum and four-momentum of meson i ($i = s\bar{s}, c\bar{c}, s\bar{c}, c\bar{s}$) by S_i , L_i and $P_i = (E_i, \vec{P}_i)$, respectively. The Mandelstam variables are $s = (E_{s\bar{s}} + E_{c\bar{c}})^2 - (\vec{P}_{s\bar{s}} + \vec{P}_{c\bar{c}})^2$ and $t = (E_{s\bar{s}} - E_{s\bar{c}})^2 - (\vec{P}_{s\bar{s}} - \vec{P}_{s\bar{c}})^2$. Let \vec{P} and \vec{P}' be the momenta of mesons A and C in the center-of-mass frame of A and B , respectively. The unpolarised cross section for the scattering in the prior form is

$$\sigma_{\text{prior}}^{\text{unpol}} = \frac{1}{(2S_{s\bar{s}} + 1)(2S_{c\bar{c}} + 1)(2L_{c\bar{c}} + 1)} \frac{1}{32\pi s} \frac{|\vec{P}'(\sqrt{s})|}{|\vec{P}(\sqrt{s})|} \sum_{SL_{c\bar{c}z}} (2S + 1) \int_0^\pi d\theta |\mathcal{M}_{\text{fi}}^{\text{prior}}(s, t)|^2 \sin \theta, \quad (1)$$

where $\mathcal{M}_{\text{fi}}^{\text{prior}}$ is the transition amplitude for the scattering in the prior form, S is the total spin of mesons A and B , $L_{c\bar{c}z}$ is the magnetic projection quantum number of $L_{c\bar{c}}$ and θ is the angle between \vec{P} and \vec{P}' . The unpolarised cross section for the scattering in the post form is

$$\sigma_{\text{post}}^{\text{unpol}} = \frac{1}{(2S_{s\bar{s}} + 1)(2S_{c\bar{c}} + 1)(2L_{c\bar{c}} + 1)} \frac{1}{32\pi s} \frac{|\vec{P}'(\sqrt{s})|}{|\vec{P}(\sqrt{s})|} \sum_{SL_{c\bar{c}z}} (2S + 1) \int_0^\pi d\theta |\mathcal{M}_{\text{fi}}^{\text{post}}(s, t)|^2 \sin \theta, \quad (2)$$

where $\mathcal{M}_{\text{fi}}^{\text{post}}$ is the transition amplitude for the scattering in the post form. The unpolarised cross section for $A(s\bar{s}) + B(c\bar{c}) \rightarrow C(s\bar{c}) + D(c\bar{s})$ is

$$\sigma^{\text{unpol}} = \frac{1}{2} (\sigma_{\text{prior}}^{\text{unpol}} + \sigma_{\text{post}}^{\text{unpol}}). \quad (3)$$

Let $\psi_{s\bar{s}}$ ($\psi_{c\bar{c}}, \psi_{s\bar{c}}, \psi_{c\bar{s}}$) stand for the product of colour, spin, flavour and relative-motion wave functions of $s\bar{s}$ ($c\bar{c}, s\bar{c}, c\bar{s}$) and V_{ab} the interaction between constituents a and b . The

transition amplitudes are given by

$$\mathcal{M}_{\text{fi}}^{\text{prior}} = 4\sqrt{E_{s\bar{s}}E_{c\bar{c}}E_{s\bar{c}}E_{c\bar{s}}}\langle\psi_{s\bar{c}}|\langle\psi_{c\bar{s}}|(V_{s\bar{c}} + V_{c\bar{s}} + V_{sc} + V_{\bar{s}\bar{c}})|\psi_{s\bar{s}}\rangle|\psi_{c\bar{c}}\rangle, \quad (4)$$

$$\mathcal{M}_{\text{fi}}^{\text{post}} = 4\sqrt{E_{s\bar{s}}E_{c\bar{c}}E_{s\bar{c}}E_{c\bar{s}}}\langle\psi_{s\bar{c}}|\langle\psi_{c\bar{s}}|(V_{s\bar{s}} + V_{c\bar{c}} + V_{sc} + V_{\bar{s}\bar{c}})|\psi_{s\bar{s}}\rangle|\psi_{c\bar{c}}\rangle. \quad (5)$$

The potential V_{ab} in coordinate space is

$$V_{ab}(\vec{r}) = V_{\text{si}}(\vec{r}) + V_{\text{ss}}(\vec{r}), \quad (6)$$

where \vec{r} is the relative coordinate of a and b , V_{si} is the central spin-independent potential and V_{ss} the spin-spin interaction. V_{si} is given by

$$V_{\text{si}}(\vec{r}) = -\frac{\vec{\lambda}_a}{2} \cdot \frac{\vec{\lambda}_b}{2} \frac{3}{4} D \left[1.3 - \left(\frac{T}{T_c} \right)^4 \right] \tanh(Ar) + \frac{\vec{\lambda}_a}{2} \cdot \frac{\vec{\lambda}_b}{2} \frac{6\pi}{25} \frac{v(\lambda r)}{r} \exp(-Er), \quad (7)$$

where $D = 0.7$ GeV, $T_c = 0.175$ GeV, $A = 1.5[0.75 + 0.25(T/T_c)^{10}]^6$ GeV, $E = 0.6$ GeV and $\lambda = \sqrt{3b_0/16\pi^2\alpha'}$ in which $\alpha' = 1.04$ GeV⁻² and $b_0 = 11 - \frac{2}{3}N_f$ with the quark flavour number $N_f = 4$. $\vec{\lambda}_a \cdot \vec{\lambda}_b$ is the product of the Gell-Mann matrices for the colour generators of a and b . The dimensionless function $v(x)$ is given by Buchmüller and Tye [9]. The short-distance part of V_{si} originates from one-gluon exchange plus perturbative one- and two-loop corrections. The intermediate-distance and large-distance part of V_{si} fits well the numerical potential obtained in the lattice gauge calculations [10]. At large distances V_{si} is independent of \vec{r} and exhibits a plateau. The plateau height decreases with increasing temperature. This means that confinement becomes weaker and weaker.

The spin-spin interaction with relativistic effects [7, 11] is [4, 12]

$$V_{\text{ss}}(\vec{r}) = -\frac{\vec{\lambda}_a}{2} \cdot \frac{\vec{\lambda}_b}{2} \frac{16\pi^2}{25} \frac{d^3}{\pi^{3/2}} \exp(-d^2 r^2) \frac{\vec{s}_a \cdot \vec{s}_b}{m_a m_b} + \frac{\vec{\lambda}_a}{2} \cdot \frac{\vec{\lambda}_b}{2} \frac{4\pi}{25} \frac{1}{r} \frac{d^2 v(\lambda r)}{dr^2} \frac{\vec{s}_a \cdot \vec{s}_b}{m_a m_b}, \quad (8)$$

where $\vec{s}_a(\vec{s}_b)$ and $m_a(m_b)$ are the spin and mass of constituent $a(b)$, respectively. The flavour dependence of the interaction is relevant to quark masses as shown in $\frac{1}{m_a m_b}$ and d ,

$$d^2 = \sigma_0^2 \left[\frac{1}{2} + \frac{1}{2} \left(\frac{4m_a m_b}{(m_a + m_b)^2} \right)^4 \right] + \sigma_1^2 \left(\frac{2m_a m_b}{m_a + m_b} \right)^2, \quad (9)$$

where $\sigma_0 = 0.15$ GeV and $\sigma_1 = 0.705$. The second term in Eq. (8) arises from the perturbative one- and two-loop corrections to the gluon propagator.

By solving the Schrödinger equation with the central spin-independent potential plus the spin-spin interaction, meson masses and quark-antiquark relative-motion wave functions are

obtained. In solving the Schrödinger equation the masses of the charm quark, the up quark and the strange quark are 1.51 GeV, 0.32 GeV and 0.5 GeV, respectively. The experimental masses of ϕ , J/ψ , ψ' , χ_c , D_s and D_s^* mesons [13] and the experimental data of S -wave $I = 2$ elastic phase shifts for $\pi\pi$ scattering in vacuum [14] are reproduced with $V_{ab}(\vec{r})$ at $T = 0$ and the quark-antiquark relative-motion wave functions.

While $V_{ab}(\vec{r})$ and the quark-antiquark relative-motion wave functions obtained from the Schrödinger equation with the potential are used to calculate $\mathcal{M}_{\text{fi}}^{\text{prior}}$ and $\mathcal{M}_{\text{fi}}^{\text{post}}$, we get $\mathcal{M}_{\text{fi}}^{\text{prior}} = \mathcal{M}_{\text{fi}}^{\text{post}}$. This is exactly what is concluded in Ref. [15] from a general argument.

With the unpolarised cross sections for charmonium dissociation we calculate the dissociation rate of charmonium in the interaction with ϕ meson in hadronic matter,

$$n\langle v_{\text{rel}}\sigma^{\text{unpol}}\rangle = \frac{3}{4\pi^2} \int_0^\infty \int_{-1}^1 d|\vec{k}| d\cos\theta \vec{k}^2 v_{\text{rel}}\sigma^{\text{unpol}} f(\vec{k}), \quad (10)$$

where n is the ϕ number density, v_{rel} is the relative velocity of the ϕ meson and the charmonium, θ is the angle between the ϕ momentum \vec{k} and the charmonium momentum and $f(\vec{k})$ is the Bose-Einstein distribution that ϕ mesons obey. The thermal average of $v_{\text{rel}}\sigma^{\text{unpol}}$ is indicated by $\langle v_{\text{rel}}\sigma^{\text{unpol}}\rangle$ [12].

III. NUMERICAL RESULTS AND DISCUSSIONS

When a ϕ meson collides with one of J/ψ , ψ' and χ_c , $D_s^- D_s^+$, $D_s^{*-} D_s^+$, $D_s^- D_s^{*+}$ or $D_s^{*-} D_s^{*+}$ is produced. Since the cross section for the production of $D_s^{*-} D_s^+$ equals the cross section for the production of $D_s^- D_s^{*+}$, they are shown in the same figure. In Figs. 1-9 we plot cross sections for the following dissociation reactions: $\phi J/\psi \rightarrow D_s^- D_s^+$, $\phi J/\psi \rightarrow D_s^{*-} D_s^+$ or $D_s^- D_s^{*+}$, $\phi J/\psi \rightarrow D_s^{*-} D_s^{*+}$, $\phi\psi' \rightarrow D_s^- D_s^+$, $\phi\psi' \rightarrow D_s^{*-} D_s^+$ or $D_s^- D_s^{*+}$, $\phi\psi' \rightarrow D_s^{*-} D_s^{*+}$, $\phi\chi_c \rightarrow D_s^- D_s^+$, $\phi\chi_c \rightarrow D_s^{*-} D_s^+$ or $D_s^- D_s^{*+}$ and $\phi\chi_c \rightarrow D_s^{*-} D_s^{*+}$. Each curve in a figure corresponds to one of the six temperatures, 0, $0.65T_c$, $0.75T_c$, $0.85T_c$, $0.9T_c$ and $0.95T_c$.

Cross sections for $A + B \rightarrow C + D$ depend on masses of mesons A , B , C and D . When temperature approaches the critical temperature T_c , D_s^\pm and $D_s^{*\pm}$ become degenerate in mass. The sum of the D_s^- and D_s^+ masses almost equals the sum of the D_s^{*-} and D_s^+ masses or the sum of the D_s^{*-} and D_s^{*+} masses at $T = 0.95T_c$. However, the cross sections for $\phi J/\psi \rightarrow D_s^- D_s^+$, $\phi J/\psi \rightarrow D_s^{*-} D_s^+$ and $\phi J/\psi \rightarrow D_s^{*-} D_s^{*+}$ are still different as shown in Figs. 1-3. This is because the spin matrix elements involved in the transition amplitude are different for the three reactions.

The two reactions $\phi J/\psi \rightarrow D_s^{*-} D_s^+$ and $\phi J/\psi \rightarrow D_s^{*-} D_s^{*+}$ are endothermic at $T/T_c = 0.75, 0.85$ and 0.9 . The sum of the D_s^{*-} and D_s^+ masses is smaller than the sum of the D_s^{*-} and D_s^{*+} masses. The square root of the Mandelstam variable $\sqrt{s_{\text{pa}}}$ corresponding to the peak cross section of $\phi J/\psi \rightarrow D_s^{*-} D_s^+$ is smaller than $\sqrt{s_{\text{paa}}}$ corresponding to the peak cross section of $\phi J/\psi \rightarrow D_s^{*-} D_s^{*+}$. The ϕ momentum \vec{P} of $\phi J/\psi \rightarrow D_s^{*-} D_s^+$ at $\sqrt{s_{\text{pa}}}$ has magnitude smaller than the one of $\phi J/\psi \rightarrow D_s^{*-} D_s^{*+}$ at $\sqrt{s_{\text{paa}}}$. Accordingly, the factor $\frac{1}{s|\vec{P}|}$ in Eqs. (1) and (2) are larger for $\phi J/\psi \rightarrow D_s^{*-} D_s^+$ than for $\phi J/\psi \rightarrow D_s^{*-} D_s^{*+}$. On the other hand, the relative momentum \vec{p}_{ab} of constituents a and b due to small $|\vec{P}|$ in $\phi J/\psi \rightarrow D_s^{*-} D_s^+$ has magnitude smaller than that in $\phi J/\psi \rightarrow D_s^{*-} D_s^{*+}$. The mesonic quark-antiquark relative-motion wave function $\psi_{ab}(\vec{p}_{ab})$ in the transition amplitude for $\phi J/\psi \rightarrow D_s^{*-} D_s^+$ is larger than the wave function for $\phi J/\psi \rightarrow D_s^{*-} D_s^{*+}$. Therefore, the peak cross section of $\phi J/\psi \rightarrow D_s^{*-} D_s^+$ is larger than the peak cross section of $\phi J/\psi \rightarrow D_s^{*-} D_s^{*+}$ at $T/T_c = 0.75, 0.85$ and 0.9 as seen in Figs. 2 and 3.

The reactions $\phi\psi' \rightarrow D_s^- D_s^+$ and $\phi\chi_c \rightarrow D_s^- D_s^+$ are exothermic below T_c . The reactions $\phi J/\psi \rightarrow D_s^- D_s^+$, $\phi\psi' \rightarrow D_s^{*-} D_s^+$ and $\phi\chi_c \rightarrow D_s^{*-} D_s^+$ are exothermic below $0.95T_c$. The threshold energy of every exothermic reaction is $m_\phi + m_{c\bar{c}}$ where m_ϕ and $m_{c\bar{c}}$ are the ϕ mass and the charmonium mass, respectively. We start calculating cross sections for exothermic reactions at $\sqrt{s} = m_\phi + m_{c\bar{c}} + 10^{-4}$ GeV and the cross sections at the energies correspond to the curve tops. Exothermic reactions take place as long as the two initial mesons overlap and even though the two initial mesons are at rest. However, the sizes of the initial and final mesons affect cross sections. In $\phi J/\psi \rightarrow D_s^- D_s^+$ the sizes of J/ψ , D_s^- and D_s^+ mesons at $T/T_c = 0, 0.65$ and 0.75 are so small that influence of confinement is small at such sizes. Increase of the J/ψ size with increasing temperature causes the cross section at $m_\phi + m_{J/\psi} + 10^{-4}$ GeV to increase. From $T/T_c = 0.75$ to 0.9 the D_s^- (D_s^+) size increases quickly and confinement becomes important. Since the plateau of $V_{\text{si}}(\vec{r})$ at large distances lowers with increasing temperature, confinement of the quark and the antiquark to form D_s^- and D_s^+ mesons becomes weaker and weaker and at $m_\phi + m_{J/\psi} + 10^{-4}$ GeV the cross section thus decreases. In the $\phi\psi'$ and $\phi\chi_c$ reactions the sizes of ϕ , ψ' and χ_c mesons are not small and the influence of confinement on combining a quark and an antiquark to form a D_s^- , D_s^+ , D_s^{*-} or D_s^{*+} meson is appreciable at such sizes. Weakening confinement reduces cross sections with increasing temperature. When temperature increases from $T/T_c = 0.75$ to 0.9 , the ϕ , ψ' and χ_c sizes increase rapidly and cross sections can thus go up. The two factors

make the cross section for each of the four $\phi\psi'$ or $\phi\chi_c$ reaction channels at the threshold energy plus 10^{-4} GeV decrease first and increase next, as shown in Figs. 4, 5, 7 and 8, while temperature changes from 0 to $0.9T_c$.

Charmonium dissociation in collision with ϕ meson has four channels. The unpolarised dissociation cross section in the dissociation-rate formula is the sum of the unpolarised cross sections for the four channels. In collision of ϕ with J/ψ (ψ' , χ_c) σ^{unpol} is the unpolarised cross section for $\phi J/\psi \rightarrow D_s^- D_s^+ + D_s^{*-} D_s^+ + D_s^- D_s^{*+} + D_s^{*-} D_s^{*+}$ ($\phi\psi' \rightarrow D_s^- D_s^+ + D_s^{*-} D_s^+ + D_s^- D_s^{*+} + D_s^{*-} D_s^{*+}$, $\phi\chi_c \rightarrow D_s^- D_s^+ + D_s^{*-} D_s^+ + D_s^- D_s^{*+} + D_s^{*-} D_s^{*+}$).

Numerical results of dissociation rates as functions of charmonium momentum are plotted in Figs. 10-12. Since the ϕ distribution function, the unpolarised cross section and the relative velocity in Eq. (10) vary with temperature, the dissociation rate depends on temperature. As temperature increases from $T/T_c = 0.65$ to 0.95 , the ϕ mass decreases and the ϕ distribution function increases. This is a factor that increases the charmonium dissociation rate. At zero charmonium momentum the slope of each curve is zero. Because ϕ mesons obey the Bose-Einstein distribution, there is a domain of \vec{k} in Eq. (10), which keeps \sqrt{s} near the threshold energy so that the unpolarised cross section contributes significantly. While the charmonium momentum increases, the domain shrinks and the dissociation rate thus decreases. Since the dissociation rates of J/ψ , ψ' and χ_c with ϕ are less than 0.00066, 0.002 and 0.0008, respectively, the charmonium suppression caused by the ϕ -charmonium dissociation is weak.

IV. SUMMARY

Using the temperature-dependent quark potential that is derived from perturbative QCD at short distances and the lattice gauge results at intermediate- and large-distances, we obtain the unpolarised cross sections in the quark-interchange mechanism and in the Born approximation. The reactions that we concern are $\phi J/\psi \rightarrow D_s^- D_s^+$, $\phi J/\psi \rightarrow D_s^{*-} D_s^+$ or $D_s^- D_s^{*+}$, $\phi J/\psi \rightarrow D_s^{*-} D_s^{*+}$, $\phi\psi' \rightarrow D_s^- D_s^+$, $\phi\psi' \rightarrow D_s^{*-} D_s^+$ or $D_s^- D_s^{*+}$, $\phi\psi' \rightarrow D_s^{*-} D_s^{*+}$, $\phi\chi_c \rightarrow D_s^- D_s^+$, $\phi\chi_c \rightarrow D_s^{*-} D_s^+$ or $D_s^- D_s^{*+}$ and $\phi\chi_c \rightarrow D_s^{*-} D_s^{*+}$. The meson masses, confinement and mesonic quark-antiquark relative-motion wave functions cause the large variation of the cross sections with respect to temperature. Medium effects on the dissociation reactions are prominent. When the confinement gives similar contributions to two reaction

channels, the spin-spin interaction makes the difference of the unpolarised cross sections for the two channels. Using the unpolarised cross sections for the 12 reactions, we obtain the dissociation rates of charmonia in the interactions with the ϕ meson. The rates generally increase with increasing temperature or with increasing charmonium momentum. The rates are quite small.

Acknowledgments

This work was supported by the National Natural Science Foundation of China under Grant No. 11175111.

-
- [1] S. G. Matinyan and B. Müller, Phys. Rev. C **58**, 2994 (1998). K. L. Haglin, Phys. Rev. C **61**, 031902 (2000). K. L. Haglin and C. Gale, Phys. Rev. C **63**, 065201 (2001). Z. Lin and C. M. Ko, Phys. Rev. C **62**, 034903 (2000); J. Phys. G **27**, 617 (2001). Y. S. Oh, T. S. Song and S. H. Lee, Phys. Rev. C **63**, 034901 (2001). F. S. Navarra, M. Nielsen and M. R. Robilotta, Phys. Rev. C **64**, 021901(R) (2001). L. Maiani, F. Piccinini, A. D. Polosa and V. Riquer, Nucl. Phys. A **741**, 273 (2004). A. Bourque and C. Gale, Phys. Rev. C **78**, 035206 (2008); Phys. Rev. C **80**, 015204 (2009).
 - [2] M. E. Peskin, Nucl. Phys. B **156**, 365 (1979). G. Bhanot and M. E. Peskin, Nucl. Phys. B **156**, 391 (1979). D. Kharzeev and H. Satz, Phys. Lett. B **334**, 155 (1994). F. Arleo, P. B. Gossiaux, T. Gousset and J. Aichelin, Phys. Rev. D **65**, 014005 (2001).
 - [3] K. Martins, D. Blaschke and E. Quack, Phys. Rev. C **51**, 2723 (1995). C.-Y. Wong, E. S. Swanson and T. Barnes, Phys. Rev. C **62**, 045201 (2000); Phys. Rev. C **65**, 014903 (2001). T. Barnes, E. S. Swanson, C.-Y. Wong and X.-M. Xu, Phys. Rev. C **68**, 014903 (2003). J. P. Hilbert, N. Black, T. Barnes and E. S. Swanson, Phys. Rev. C **75**, 064907 (2007).
 - [4] J. Zhou and X.-M. Xu, Phys. Rev. C **85**, 064904 (2012).
 - [5] S.-T. Ji, Z.-Y. Shen and X.-M. Xu, J. Phys. G **42**, 095110 (2015).
 - [6] C.-Y. Wong, Phys. Rev. C **65**, 034902 (2002).
 - [7] T. Barnes and E. S. Swanson, Phys. Rev. D **46**, 131 (1992). E. S. Swanson, Ann. Phys. (N.Y.) **220**, 73 (1992).

- [8] Y.-Q. Li and X.-M. Xu, Nucl. Phys. A **794**, 210 (2007).
- [9] W. Buchmüller and S.-H. H. Tye, Phys. Rev. D **24**, 132 (1981).
- [10] F. Karsch, E. Laermann and A. Peikert, Nucl. Phys. B **605**, 579 (2001).
- [11] S. Godfrey and N. Isgur, Phys. Rev. D **32**, 189 (1985).
- [12] X.-M. Xu, Nucl. Phys. A **697**, 825 (2002).
- [13] K. A. Olive *et al.*, Particle Data Group, Chin. Phys. C **38**, 090001 (2014).
- [14] E. Colton *et al.*, Phys. Rev. D **3**, 2028 (1971). N. B. Durusoy *et al.*, Phys. Lett. B **45**, 517 (1973). W. Hoogland *et al.*, Nucl. Phys. B **126**, 109 (1977). M. J. Losty *et al.*, Nucl. Phys. B **69**, 185 (1974).
- [15] N. F. Mott and H. S. W. Massey, *The Theory of Atomic Collisions* (Clarendon Press, Oxford, 1965). T. Barnes, N. Black and E. S. Swanson, Phys. Rev. C **63**, 025204 (2001). C.-Y. Wong and H. W. Crater, Phys. Rev. C **63**, 044907 (2001).

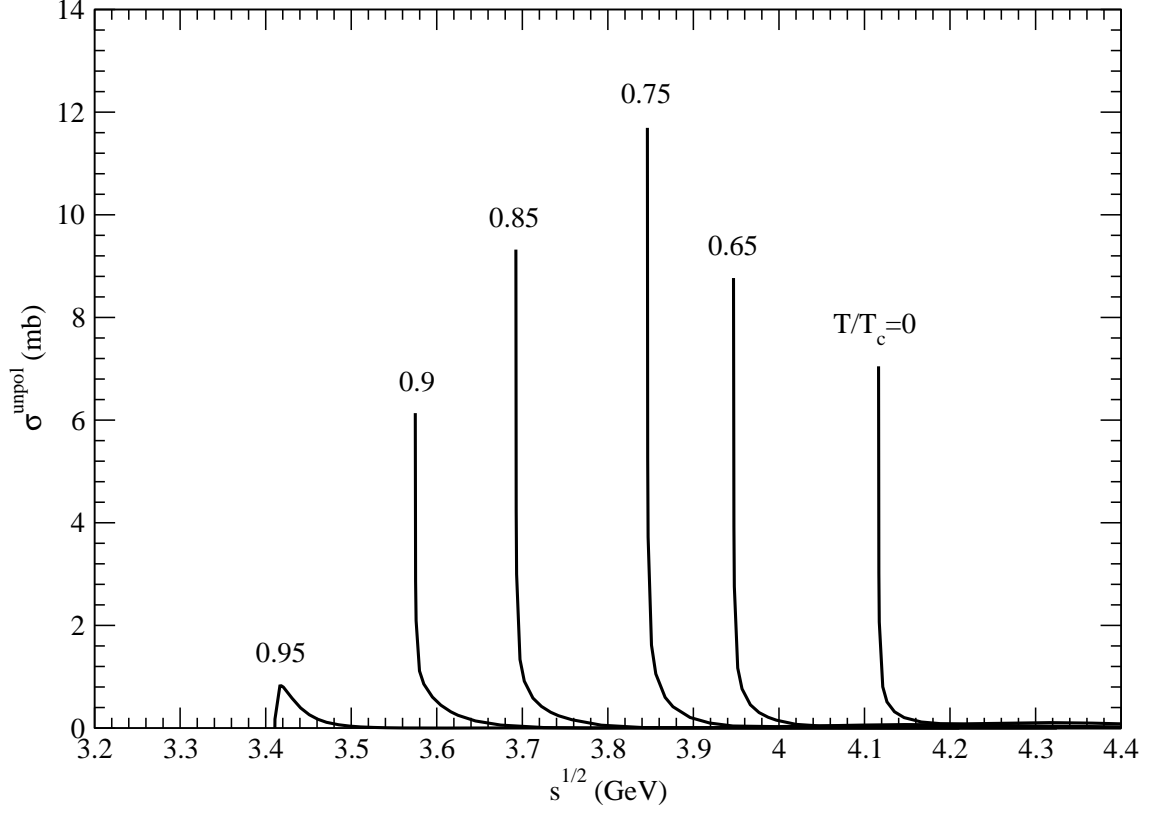


FIG. 1: Cross sections for $\phi J/\psi \rightarrow D_s^- D_s^+$ at various temperatures.

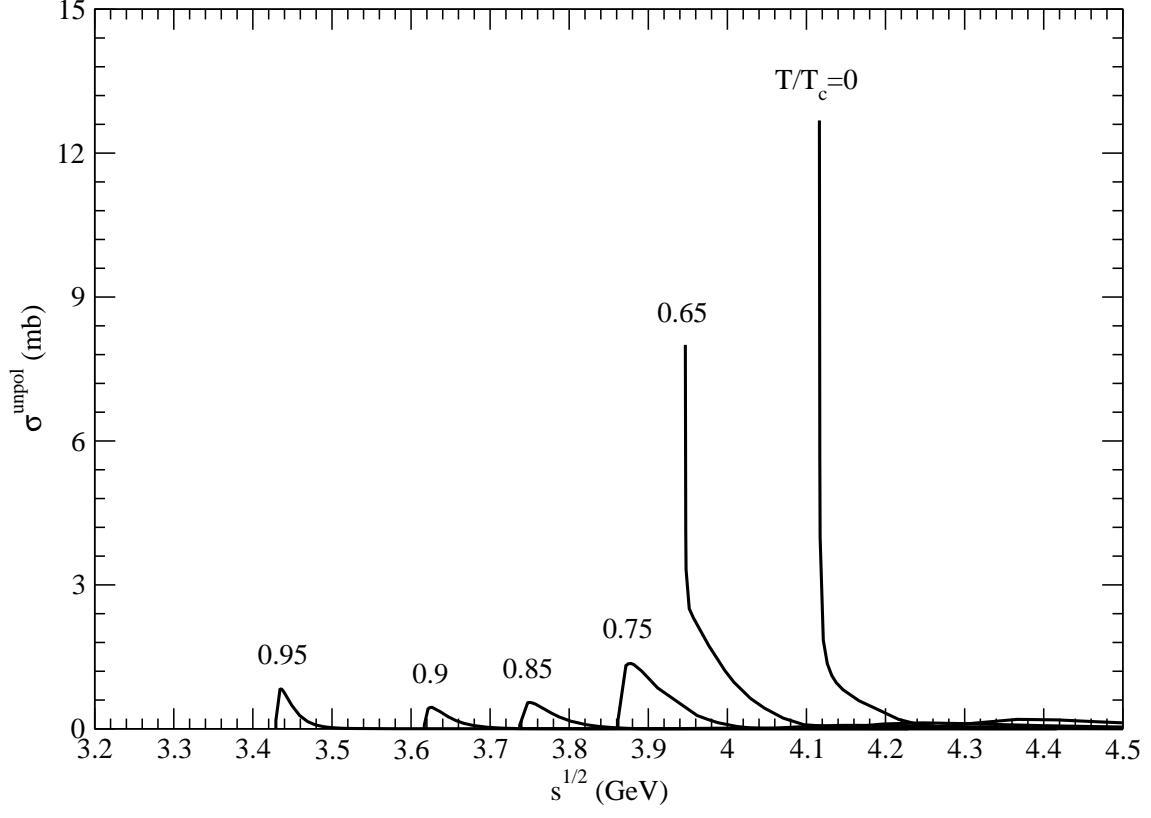


FIG. 2: Cross sections for $\phi J/\psi \rightarrow D_s^{*-} D_s^+$ or $D_s^- D_s^{*+}$ at various temperatures.

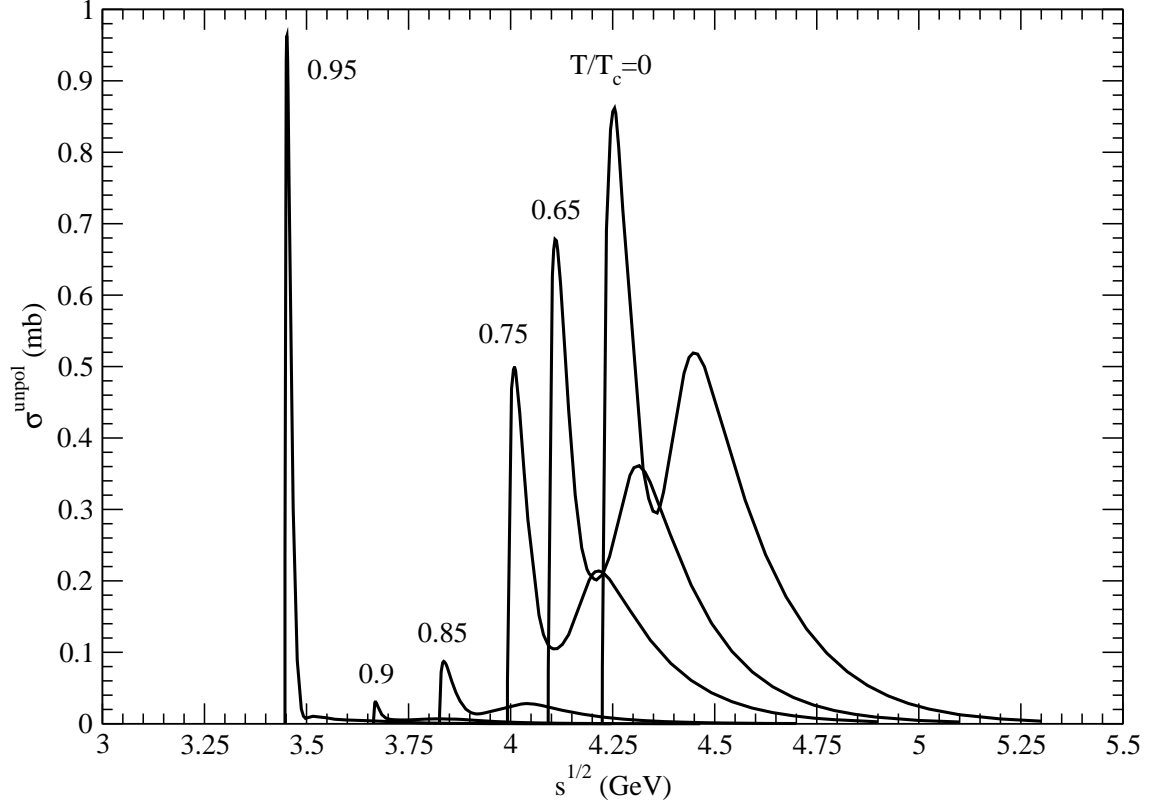


FIG. 3: Cross sections for $\phi J/\psi \rightarrow D_s^{*-} D_s^{*+}$ at various temperatures.

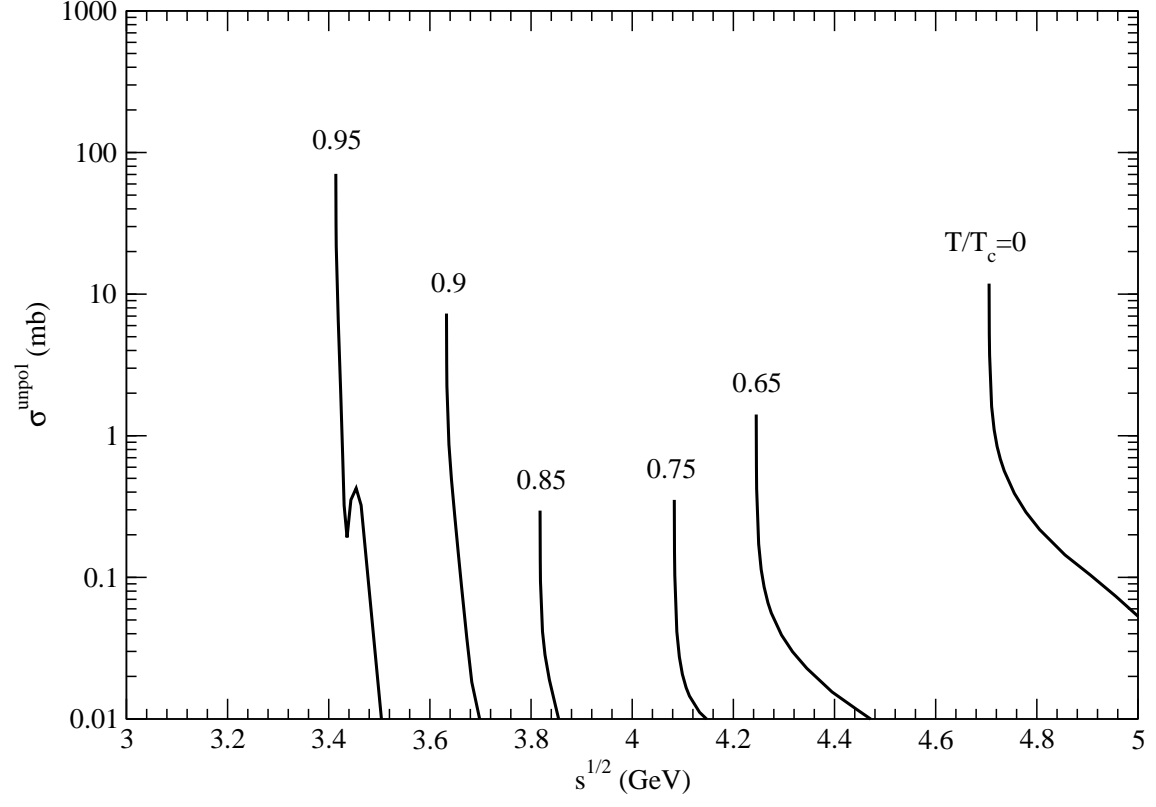


FIG. 4: Cross sections for $\phi\psi' \rightarrow D_s^- D_s^+$ at various temperatures.

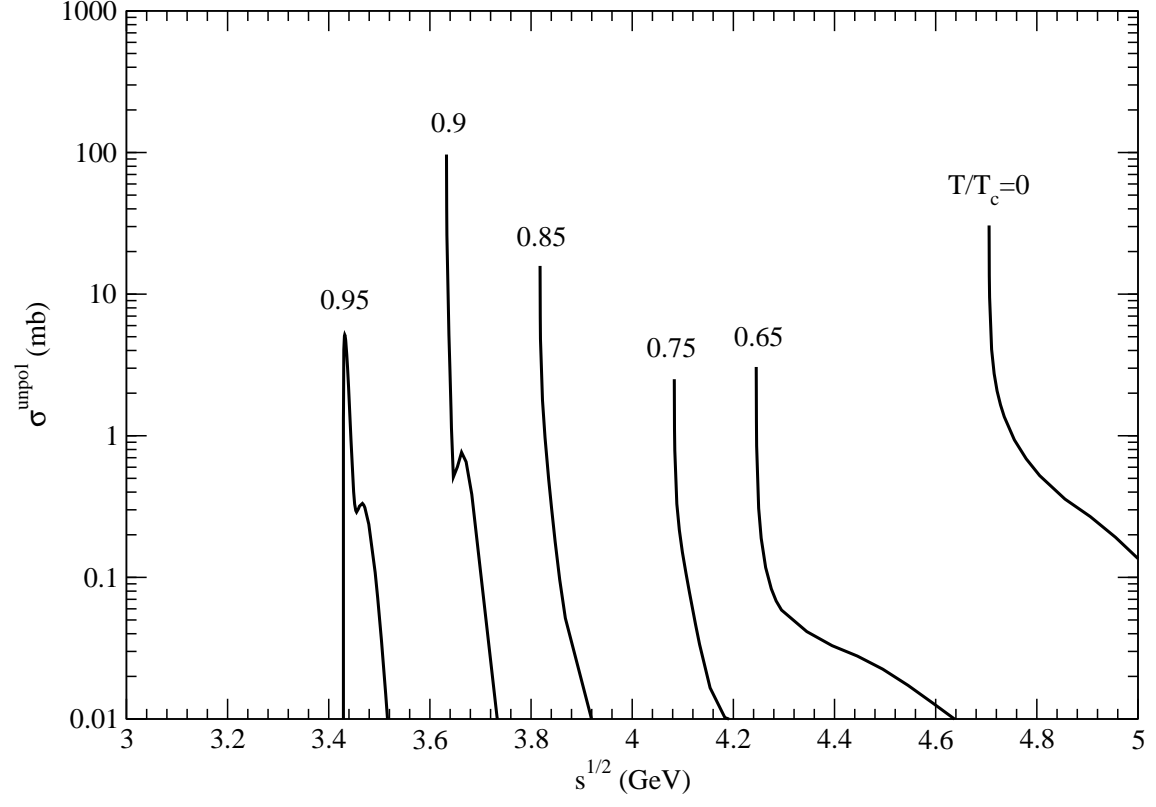


FIG. 5: Cross sections for $\phi\psi' \rightarrow D_s^{*-}D_s^+$ or $D_s^-D_s^{*+}$ at various temperatures.

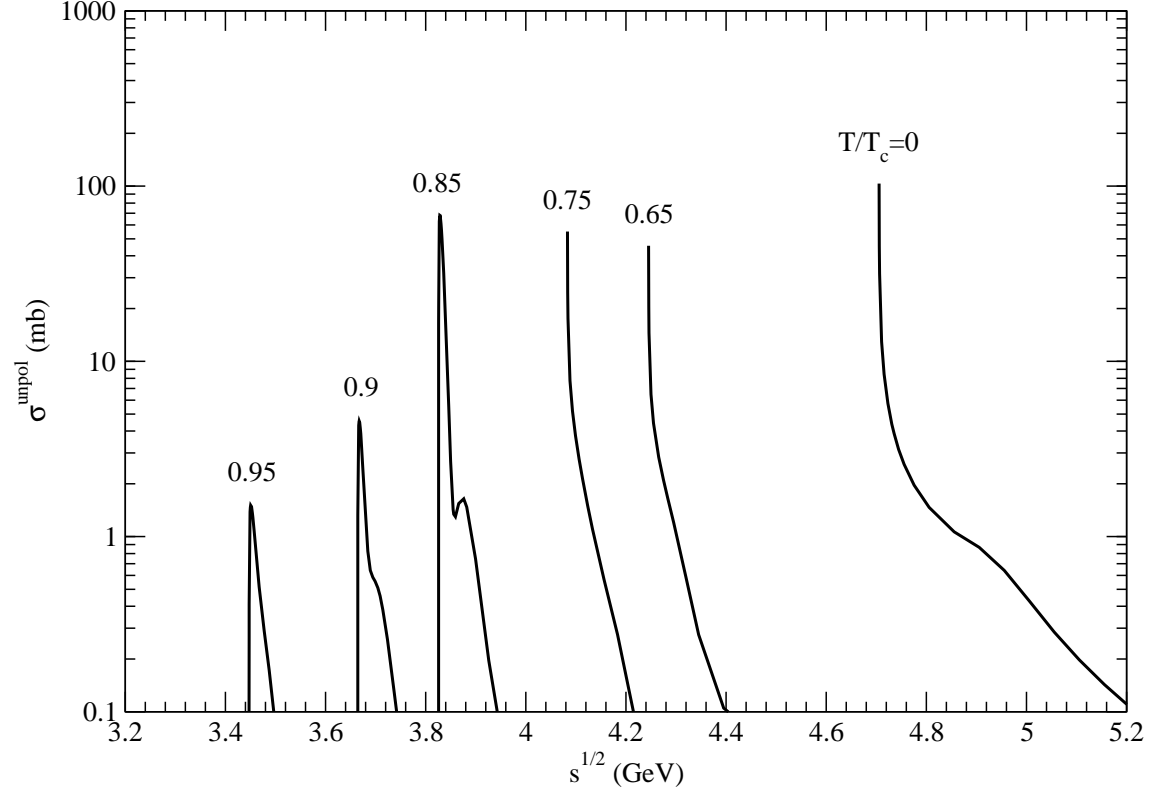


FIG. 6: Cross sections for $\phi\psi' \rightarrow D_s^{*-}D_s^{*+}$ at various temperatures.

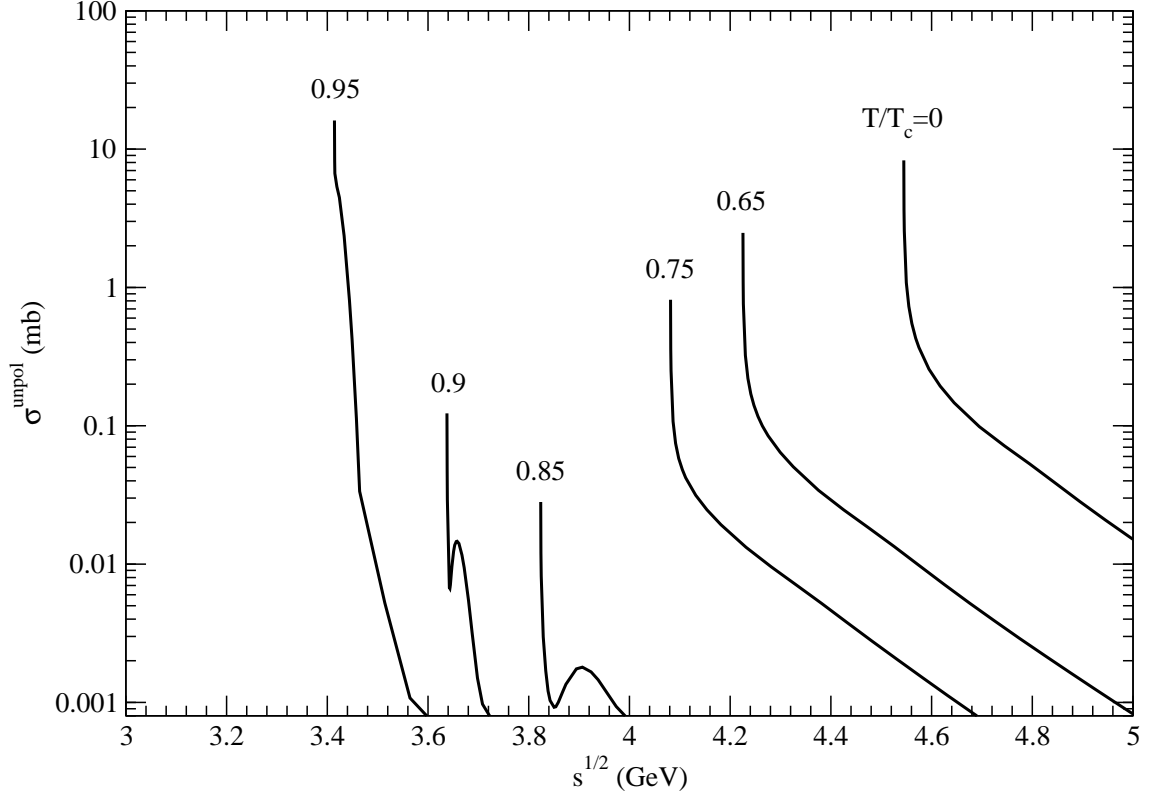


FIG. 7: Cross sections for $\phi\chi_c \rightarrow D_s^- D_s^+$ at various temperatures.

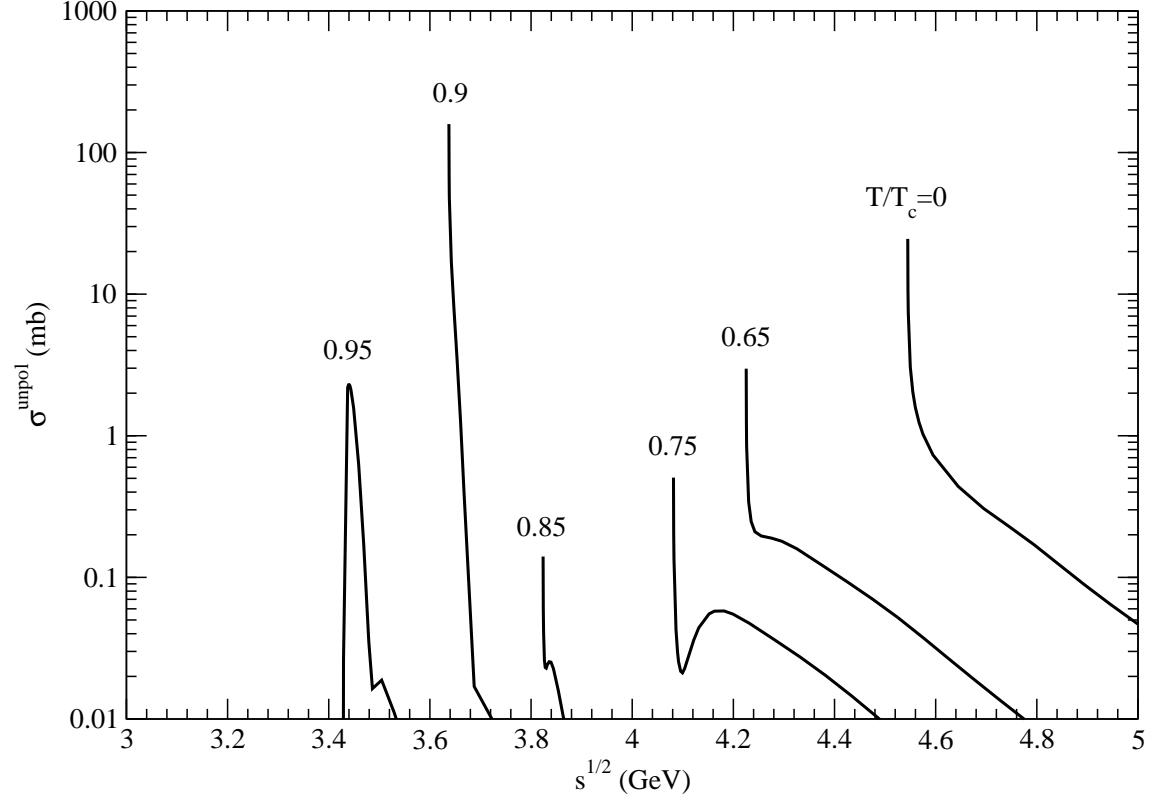


FIG. 8: Cross sections for $\phi\chi_c \rightarrow D_s^{*-}D_s^+$ or $D_s^-D_s^{*+}$ at various temperatures.

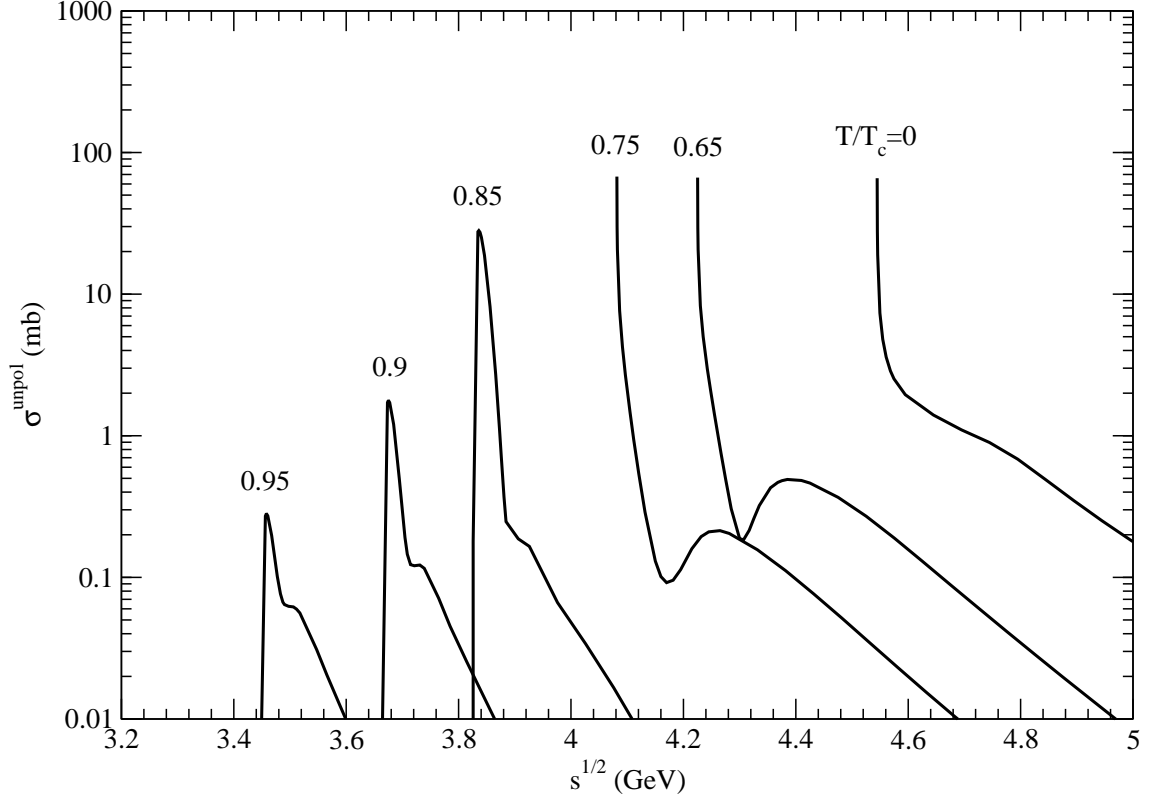


FIG. 9: Cross sections for $\phi\chi_c \rightarrow D_s^{*-}D_s^{*+}$ at various temperatures.

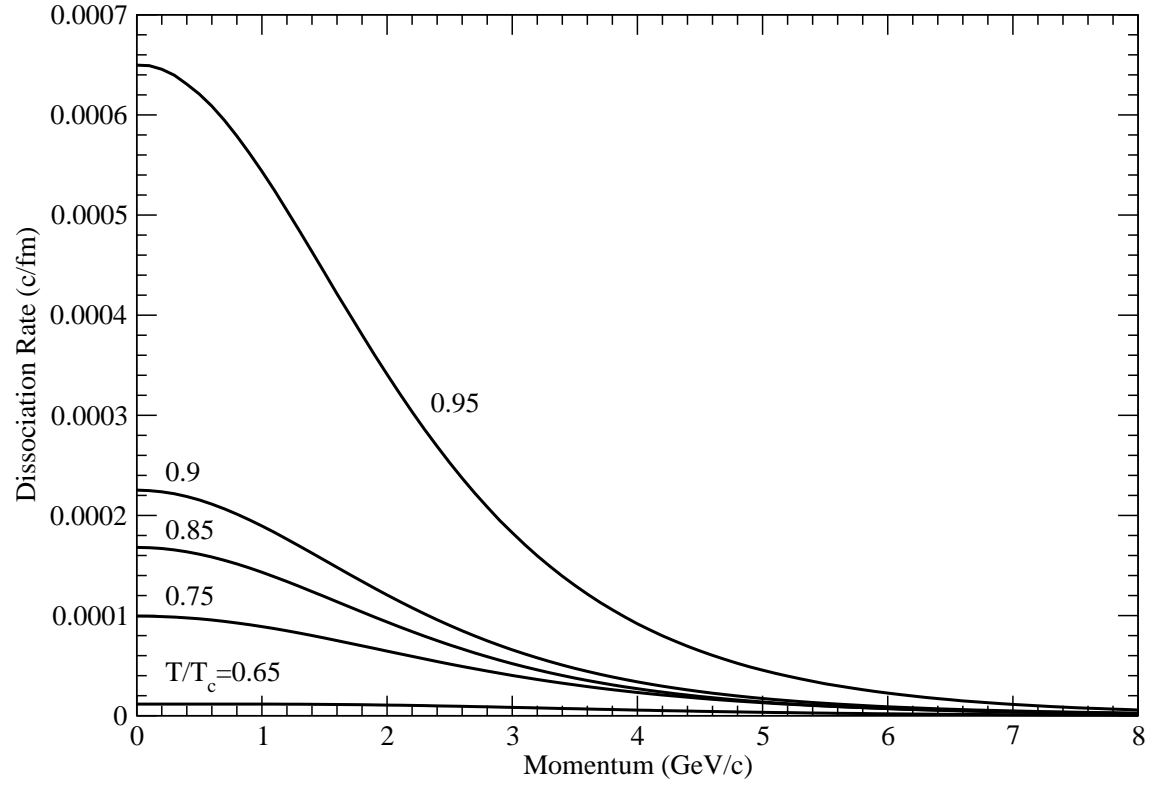


FIG. 10: Dissociation rate of J/ψ with ϕ versus the J/ψ momentum at various temperatures.

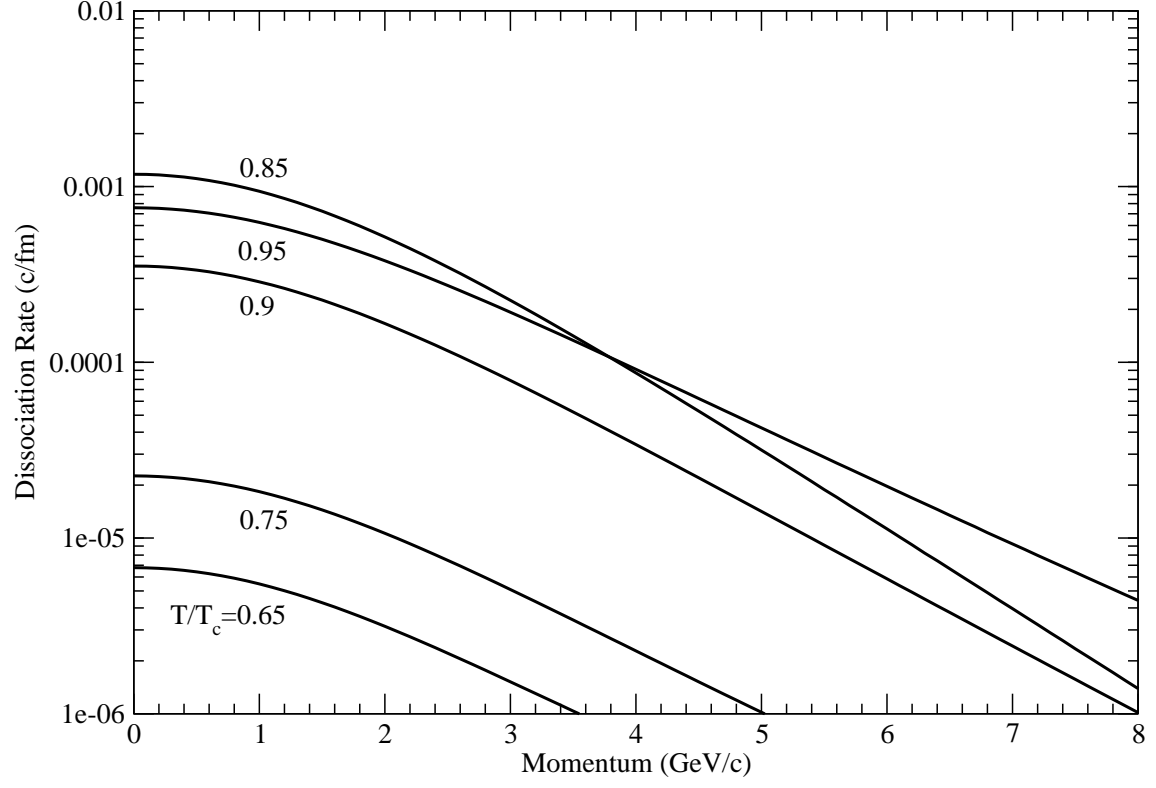


FIG. 11: Dissociation rate of ψ' with ϕ versus the ψ' momentum at various temperatures.

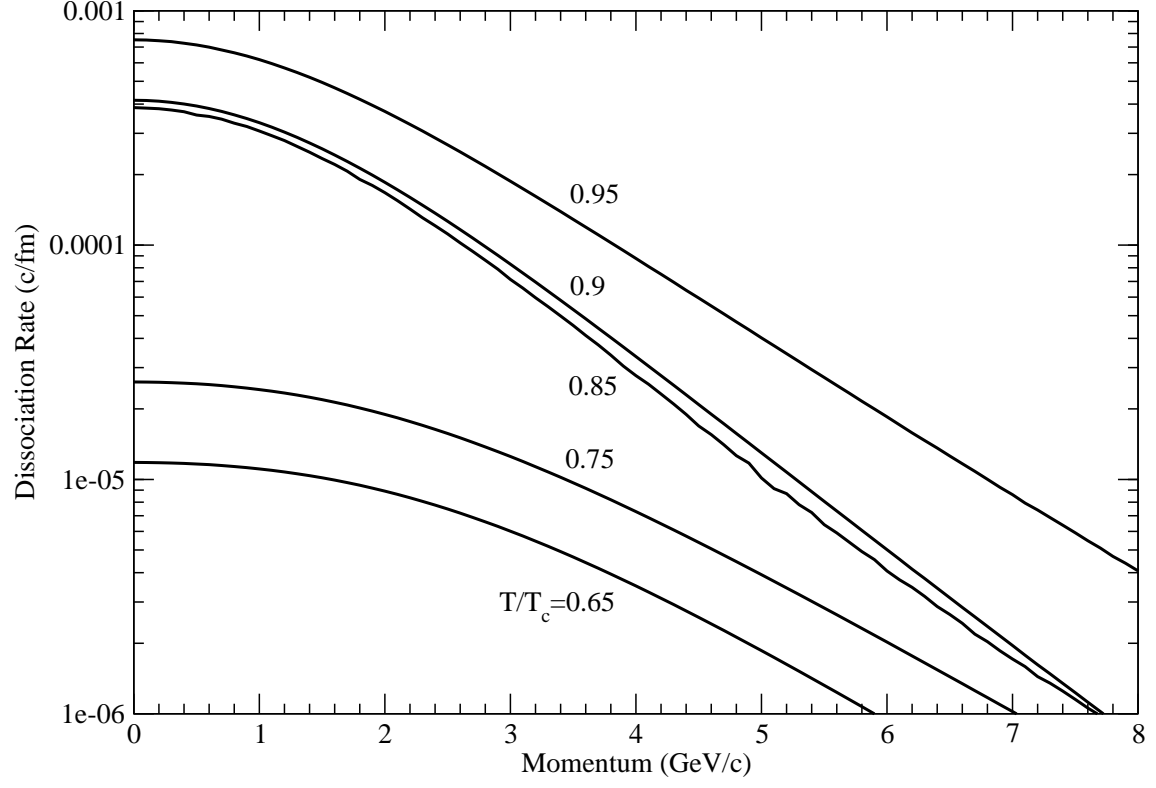


FIG. 12: Dissociation rate of χ_c with ϕ versus the χ_c momentum at various temperatures.